



Since January 2020 Elsevier has created a COVID-19 resource centre with free information in English and Mandarin on the novel coronavirus COVID-19. The COVID-19 resource centre is hosted on Elsevier Connect, the company's public news and information website.

Elsevier hereby grants permission to make all its COVID-19-related research that is available on the COVID-19 resource centre - including this research content - immediately available in PubMed Central and other publicly funded repositories, such as the WHO COVID database with rights for unrestricted research re-use and analyses in any form or by any means with acknowledgement of the original source. These permissions are granted for free by Elsevier for as long as the COVID-19 resource centre remains active.

Infrared Thermography and Soft Computing for Diabetic Foot Assessment

Sudha Bandalakunta Gururajao*, Umadevi Venkatappa*, Joshi Manisha Shivaram*, Mohamed Yacin Sikkandar[†], Abdullah Al Amoudi[†]

*B.M.S. College of Engineering, Bangalore, India, [†]College of Applied Medical Sciences, Majmaah University, Al Majmaah, Kingdom of Saudi Arabia

1 Introduction

Medical infrared thermography (MIT) is a technology which has its roots dating back to 400 BC when, change in body heat was considered as an indication of an underlying medical condition [1]. The following section is a briefing of infrared thermography and related terms.

Infrared thermography is a graphical representation of heat.

Thermogram: The picture produced by infrared thermography, using photographic film sensitive to infrared radiation or the record produced by a thermograph.

Radiation: Transfer of energy through electromagnetic waves.

The types of thermography are contact thermography (using liquid crystals), remote sensing thermography (using IR optical and detector system) and computer assisted thermography (using modern robust thermal imaging cameras) [1–3]. Different types of imaging methods based on infrared radiation are static, dynamic (DAT, subtraction), dynamic (active), TTM (thermal texture mapping), multispectral/hyperspectral, multimodality, and sensor fusion.

Medical infrared thermography (MIT) has gained importance in the recent years because of the following factors:

1. Thermal imaging is less sensitive to light and hence poor illumination does not pose any adverse effect on the image.
2. Temperature as a tool for diagnosis has shown promising results in the early detection of many diseases like breast cancer, rheumatoid arthritis, osteoarthritis, Raynaud's syndrome, and so on.

3. Surface temperature distribution of an object under study can be easily obtained over a wide area in just one click of a thermal imager.
4. The patients are not subject to any harmful radiation from the imaging equipment as infrared thermography is noninvasive, noncontact, and nonradiant.
5. With the improvements in thermal sensing equipment and software image processing capabilities, computer aided diagnostic system is feasible and accurate.

2 Characteristics of Thermal Infrared Images

Infrared radiation is an electromagnetic wave emitted by any object above absolute zero. It is just next to the visible spectra in the electromagnetic spectrum with its wavelength in the range 0.7 to 1000 μm .

The important characteristics of thermal infrared images are resolution, noise, spectrum, and dynamic range.

2.1 Spatial Characteristics (Resolution)

Fig. 1 shows the thermal infrared sensing detectors (focal plane array) of dimension 320×240 producing a thermal image of 320×240 pixels. The thermal infrared image is shown in Fig. 2. Each pixel in the image shows the surface temperature detected at that point. Thus the image represents the temperature distribution across the surface of the object imaged. The variation in temperature is depicted using different colors as seen in the temperature scale. Here dark color represents lower temperature and light color higher temperature.

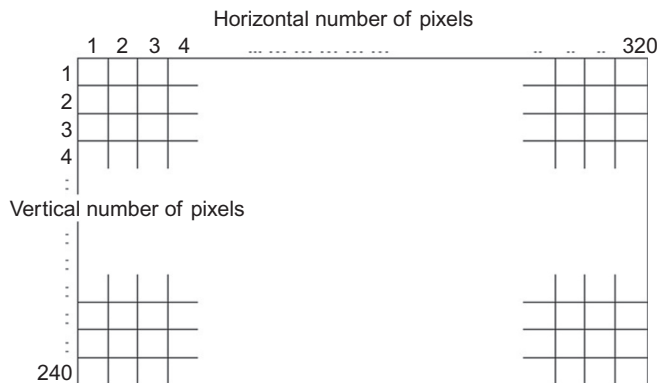


Fig. 1

Arrangement of infrared detector array corresponding to pixels in the thermal image.

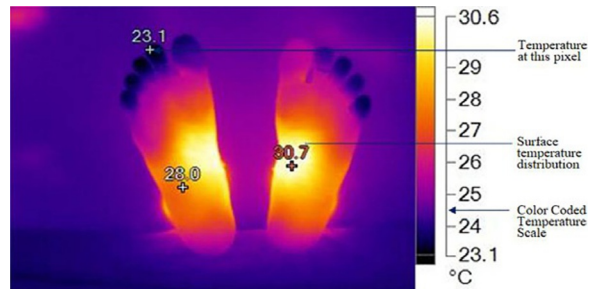


Fig. 2

Thermal image showing the spatial characteristics of the thermal image (spatial resolution 320×240 pixels).

2.2 Noise (Thermal Resolution)

Noise in the thermal image limits the camera sensitivity to detect targets of weak contrast. This is characterized by noise equivalent temperature difference (NETD) and minimum resolvable temperature difference (MRTD).

Good sensitivity and pixel count ensures that the image contains good thermal and spatial detail and hence good diagnostic ability.

2.3 Spectral Characteristics

The entire spectral band of Infrared is subdivided into five regions based on the wavelength range. The wavelength of near infrared (NIR) is between 0.7 and $1.0 \mu\text{m}$, short wave infrared is between 1 and $3 \mu\text{m}$, mid wave infrared between 3 and $5 \mu\text{m}$, long wave infrared between 8 and $14 \mu\text{m}$ and very long wave infrared having wavelength > 14 upto $1000 \mu\text{m}$.

The spectrum we are concerned lies in the long wave infrared (LWIR) region corresponding to $8\text{--}14 \mu\text{m}$ as human body radiates most at $10 \mu\text{m}$.

Higher temperatures mean higher wavelengths and thus in the thermal infrared image, hot areas are shown bright and at very high temperatures, the region is shown as white because of the emission of green and blue light at higher wavelengths. Human skin has an emissivity in the range of 0.98 which matches the emissivity of a perfect blackbody. Hence a modern day thermal imager with high sensitivity to infrared radiation can effectively measure the temperature of the object imaged. Also it has been shown that there is a correlation between the temperature of the object and the infrared energy radiated from the surface of the object.

2.4 Dynamic Range

It represents the capability of the camera to maintain the finer radiometric measurements even when the temperature spans a large range in the image captured. So a captured thermal infrared image should not have temperatures varying by $>30^\circ\text{C}$ as pointed out in Ref. [3].

The nominal for medical infrared thermography is 12 bits per pixel. The typical characteristics of a thermal image and testing of the same is explained by Houdas and Ring [4].

3 Medical Infrared Thermography

Ring [5] has studied the development of temperature measurement in medicine and the use of thermography to visualize the spatial and temporal patterns of surface temperature of man in states of health and disease over a period of 25 years. During 1934 to 1936, Hardy [6, 7] studied the physiological role of infrared emission from human body and proposed that human skin can be considered as a blackbody radiator. This heat radiation from the body surface can be detected through the use of a thermal imaging camera. Ring et al. has presented in detail the physics behind infrared thermal imaging in Ref. [8]. Thermal infrared imaging works by capturing the infrared radiation emitted from various regions of the body as temperature readings spontaneously. Every part of the body has a specific thermal pattern associated with it based on the microcirculation near skin surface. Thus thermal imaging can be used to monitor the changes in the temperature profile of a particular region with respect to time.

3.1 Early Diagnosis Using Medical Infrared Thermography

The quantification of medical infrared thermal images for early diagnosis of human pathological conditions has been attempted by many researchers as presented in Ref. [9]. The list of diseases where digital infrared thermal imaging (DITI) is used is given in Table 1.

There are many successful computational techniques in diagnosis and detection of medical conditions such as breast cancer [10] as shown in Fig. 3A and B, diabetic foot and osteoarthritis, in effectively screening potential severe acute respiratory syndrome (SARS) patients, in the analysis of cortical perfusion during ischemic strokes, in the segmentation of the eye and cornea and also in the detection of glaucoma from ocular thermographic images as observed in Ref. [11].

A typical diagnostic system using medical infrared thermography, image processing, and soft computing is shown in Fig. 4.

Table 1 List of medical conditions where DITI is used

<ul style="list-style-type: none"> • Breast cancer • Diabetic foot ulcer and neuropathy detection • Lung cancer • Arthritis • Sports injury 	<ul style="list-style-type: none"> • Glaucoma • Dental abscess • Blood perfusion • Skin lesions • Respiratory distress • Raynaud's phenomenon
--	---

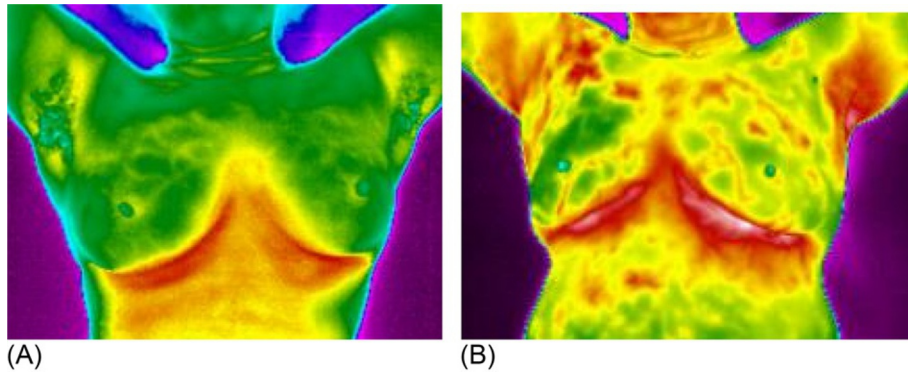


Fig. 3
(A) Normal breast and (B) abnormal breast.

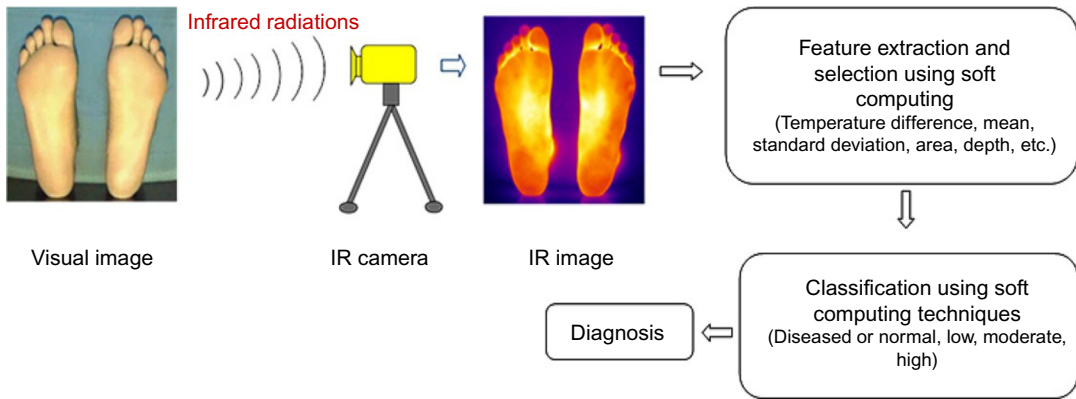


Fig. 4
Block diagram showing the typical use of soft computing and infrared thermography for medical diagnosis.

3.2 How Is IR Thermal Imaging Different From Other Medical Imaging Modalities?

An IR thermal image captures the infrared energy radiated from the surface of the skin or any other object above absolute zero. The salient feature of thermography is its ability to image the thermovascular appearance of the skin and not the structure and anatomy of the human body which is done by many other medical imaging modalities. Jones and Plassman [12] details the journey of the improvements in thermal imagers, how an IR image is formed, processed, and analyzed for detective the changes in response to different stimuli like cool temperatures. Izhar in his thesis [13] describes the registration and analysis of thermal images in medicine. Oliver Faust et al. [14] have given a review of algorithms used for computer aided diagnosis systems using thermography. But most of these do not make use of soft computing techniques for the processing of the infrared thermal images.

Herry and Frize in their work [15] present techniques to de-noise the infrared images, to remove the background from the infrared images to identify the regions of interest and statistical analysis of the ROIs to classify normal and abnormal temperatures.

3.3 Role of Soft Computing in Medical Infrared Thermography

Modern intelligent diagnostic systems for medical thermal infrared image analysis is built on a combination of various soft computing techniques such as fuzzy logic (FL), neurocomputing (NC), evolutionary computing (EC), probabilistic computing (PC), and parts of machine learning (ML). These techniques include artificial neural networks (ANN), fuzzy-C-means (FCM), deep learning—convolutional neural networks (CNN), support vector machine (SVM), genetic algorithm (GA), fuzzy neural networks, and Bayesian networks. SVM and ANN rule this space and with the improvement in hardware and computing capability like graphical processing units (GPU), deep learning architectures are paving way for more accurate intelligent systems. A lot of hybrid soft computing techniques have been used for medical thermal infrared image analysis. For a more detailed understanding of soft computing techniques for medical image analysis please refer [16].

4 Main Focus and Motivation Behind the Chapter

This chapter focuses on the use of medical infrared thermography and soft computing particularly deep learning for diabetic foot assessment. Diabetic foot complications are a major cause of concern for diabetic patients as it affects mobility and quality of life. At present, any patient suffering from diabetes for five or more years in the case of type 1 diabetes and patients diagnosed with type 2 should undergo foot evaluation to prevent any foot complication such as ulcer or peripheral neuropathy. This requires the patient to visit the foot evaluation clinic in regular periods usually 3 months in the case of at risk patients, 6 months with patients involving other diabetic complications and peripheral arterial disease and 1 year for regular foot evaluation. This is cumbersome looking at the money and time involved. Many patients avoid or ignore the visit. This later converts to foot or toe amputation which can be avoided if computer aided diagnosis system is available at home as an app in mobile or for telemedicine purposes. For such a system, image processing has to be done automatically and abnormality has to be detected immediately that suggests treatment or visiting the clinic. This is where machine learning comes into play as image processing for the extraction of abnormal regions, grading the level of complication and for decision making to suggest further action such as suggesting the patient to visit the foot evaluation clinic and get the treatment done or later for telemedicine. Hence we studied the surface temperature distribution (STD) patterns in the plantar foot of both diabetic and healthy subjects to establish the differences in temperature capable to early diagnosis of the complication and we are looking forward to building a diagnostic system to detect and assess diabetic foot complications early to prevent amputation.

The broad objective of this research is to design an intelligent system to auto detect the onset and assessment of foot complications caused by diabetes and to improve the early diagnosis of the same. It is based on the analysis of IR thermal images of the regions of interest of the foot. The main objectives are

- (1) Study of surface temperature distribution in the plantar foot of diabetic and normal subjects to evaluate the potential of thermography for early diagnosis of type 1 and type 2 diabetic complications.
- (2) Design of an automated intelligent assessment system for diabetic foot complications using the aid of digital image processing techniques and artificial neural networks.
- (3) Correlation between the existing clinical methods for foot evaluation and the evaluation done by thermography will be carried out to establish the usefulness and accuracy of the system built.

5 Literature Review on Diabetic Foot Complications Assessment Using MIT

Bagavathiappan et al. [17] have studied the correlation between diabetic neuropathy and plantar foot temperature proving the capability of thermography in detecting diabetic neuropathy. Brånemark et al. [18] observed the temperature distribution patterns of hands and feet for both nondiabetic and diabetic subjects. Bharara et al. [19] formed a healing wound index based on the thermal profile of foot wound of diabetic patients. This helps in studying the healing pattern of the diabetic foot complication to suggest treatment. Peregrina-Barreto et al. [20] studied the temperature pattern of diabetic patients and have analyzed the same using angiosome concept. They have divided the entire foot into four regions corresponding to four angiosomes, a concept derived by Nagase et al. Estimated temperature difference between the left and right foot was calculated to carry out the analysis. Also, the classification of the thermal patterns is done for each of the four regions based on seven classes derived. They concluded that the estimated temperature difference did not show any difference useful for analysis and that the HSE (hot spot estimator) was capable of detecting hot spots which would turn out to be ulcer later which the ETD (estimated temperature difference) was not able to. Hernandez-Contreras et al. [21] were able to observe the butterfly pattern associated with nondiabetic subjects. They formulated an index called the TCI (thermal change index) based on the temperature readings of the corresponding angiosomes of diabetic and nondiabetic subjects. They concluded that a change of 1°C was sufficient to identify various thermal classes. No statistical analysis was done for the data. Liu et al. [22] were able to detect abnormal regions in the foot of diabetic patients using the temperature difference between the ipsilateral and contralateral foot with a cutoff of 2.2°C. Automatic segmentation and registration of the foot was carried out and then the temperature difference between the left and right foot was calculated. But the methodology followed to calculate the temperature difference was not explained. In this work, a new methodology is proposed to analyze accurately the temperature distribution in healthy and diabetic subjects. Renero-C [23] has observed abrupt changes

in temperature using thermography to detect possible diabetic foot ulcer formations. Gatt et al. [24] demonstrate that the probability of complications of PAD, neuropathy, and/or neuroischaemia being present increases as the temperature of these regions rises. A narrative review on the various techniques used for diabetic foot complications based on asymmetry analysis, stress test and temperature distribution analysis is given by Hernandez-Contreras et al. [25].

5.1 Methodology

The work done so far is shown in the flow chart (Fig. 5).

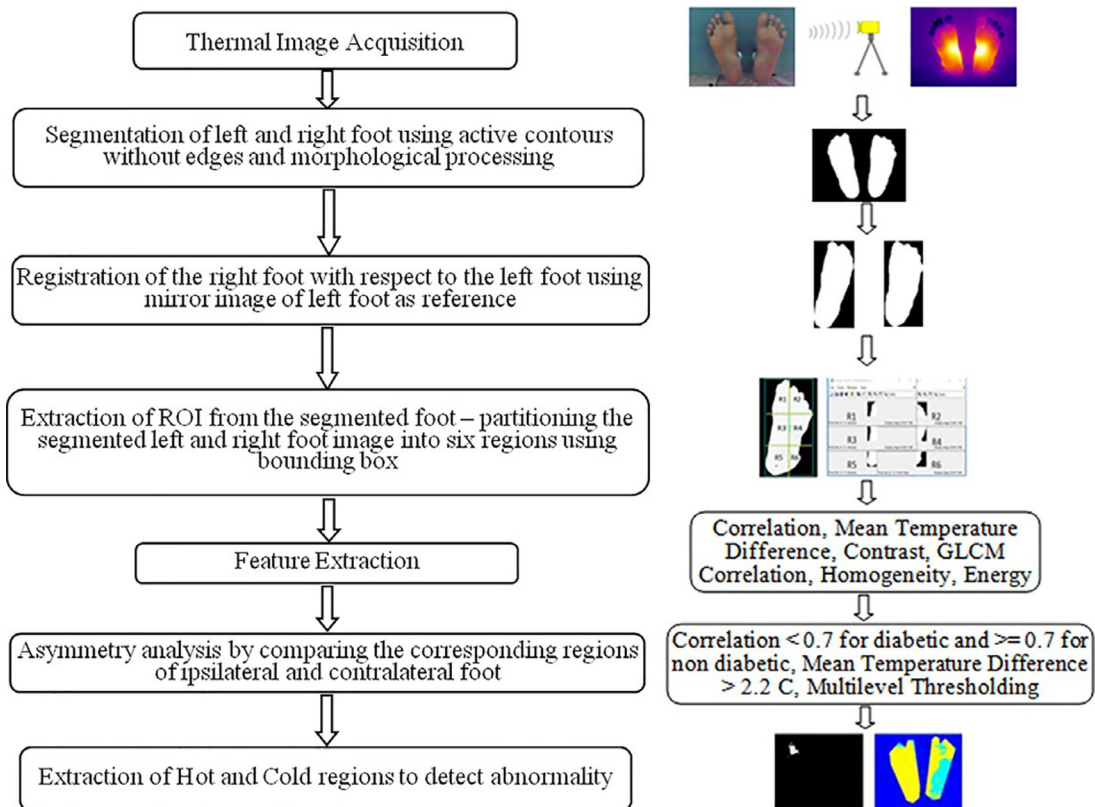


Fig. 5

Extraction of abnormal regions in plantar surface of foot.

5.2 Study Population

Sixty-two diabetic patients (38 male and 24 female) and with diabetes mellitus, and 20 nondiabetic subjects with an average age of 42 years, standard deviation 12 years. Few patients had or was having diabetic foot complications and other patients had healthy foot. We imaged the diabetic subjects at the Karnataka Institute of Endocrinology and Research (KIER), Bangalore, India after taking informed consent for the study. KIER's Institutional Ethical Committee approved the study. So, all ethical considerations were met.

Inclusion criteria

- Adult male or female, 18 years of age or over.
- Diagnosed with type 1 or type 2 diabetes.
- Is healthy without diabetes.
- Currently receiving treatment for a diagnosis of diabetic foot ulcer or have had an active foot ulcer healed within the last 6 months.
- Is willing and able to provide informed consent indicating that they understand the purpose and procedures required for the study.

Exclusion criteria

- Subjects who do not meet the inclusion criteria.
- Is currently enrolled in another clinical trial.

5.3 Thermal Image Acquisition and Segmentation

Image acquisition protocol plays an important role in infrared thermography. IR thermal image or the thermogram acquisition should be done in a controlled environment after considering the various factors briefed in Ref. [26]. IR thermal image acquisition of human foot is discussed in Ref. [27] where the different imaging setups for thermal infrared image acquisition of foot and its influence on the accuracy of the segmentation of the foot for further analysis to detect diabetic foot ulcer is analyzed.

The healthy subjects were imaged in the college laboratory and the diabetic subjects were imaged at KIER (Karnataka Institute of Endocrinology and Research, Bangalore). Informed consent was taken from all the patients involved in the study.

The thermal images of healthy foot are segmented using the method (Otsu thresholding followed by morphological processing) explained by Sudha et al. [27]. For diabetic patients, active contours without edges method for segmentation given by Chan and Vese [28] is used. If the segmented region extends beyond the edges of foot, it is removed using morphological processing. The morphological operation used is closing.

For colder toes and for diabetic patients with amputation, the aforesaid methods do not work well. For such images, roipoly function in MATLAB is used to interactively segment the

left and the right foot approximated by a polygon. This morphological processing is similar to the process discussed in Ref. [29] by Zohora et al.

But the problem in the segmentation method [27] was the segmentation of the toes region when it was cold and when the subjects had existing complications like ulcer. Hence we explored another acquisition procedure where we had cut two holes in the polyurethane foam with density 30kg/m^3 at the bottom of the foam. This made sure that patients need not insert their foot in the holes as required previously but to just keep the foam on the ankle region from the top when the subjects are lying in supine position as seen in Fig. 6. The foot is segmented automatically using a mask fixed in position for the left foot and right foot as shown in Fig. 7A and B. Then supplying this mask to the active contours function, the foot is segmented as shown in Fig. 7C.

The main advantage of using a left and right mask for segmentation is to automate the process of segmentation of the foot for all images contained in a folder. All the images obtained on a particular day are saved in the same folder. We have written a matlab script to read the images, save it in a variable and using the mask defined. This saves lot of time and energy when

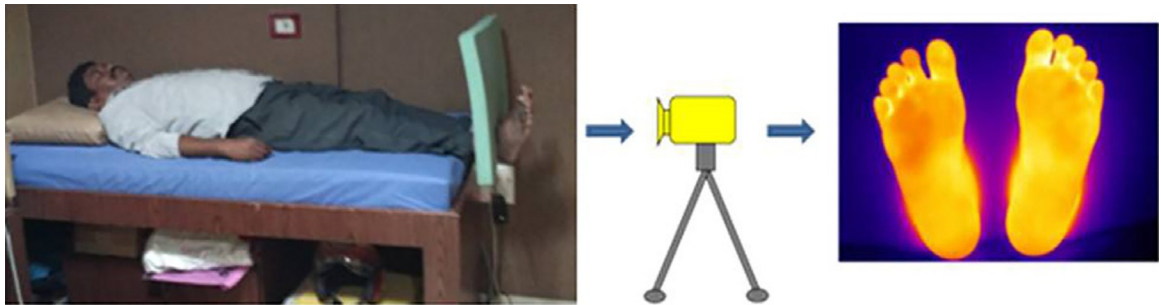


Fig. 6
Foot thermal image acquisition.

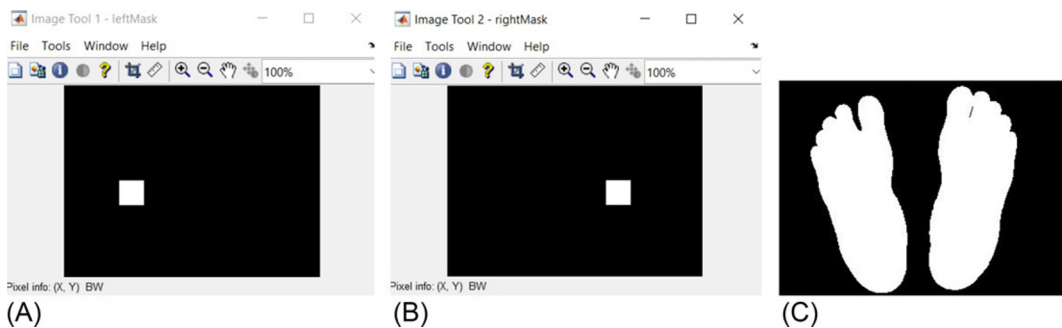


Fig. 7

(A) Initial predefined left mask, (B) right mask, and (C) segmented foot using the mask and active contours method.

compared to manual or semiautomated segmentation where human intervention is required to define the initial contour for segmentation. The segmented foot is also saved in the same folder with the same filename as the thermal image with “_mask” added to the filename.

5.4 Thermal Image Registration

Now the segmented feet are not the exact same mirror images of each other since both are not aligned with respect to each other as can be seen in Fig. 8A. The left and right foot has to be aligned to do the comparison of the temperature values. Hence, both the foot has to be registered to do the same. This is done using the following process. The mirror image of the segmented right foot is computed. Using this as the reference image, the left foot is registered. The registered left foot can be seen in Fig. 8B as magenta colored foot

5.5 Extraction of Region of Interest (ROI)

Once we have the segmented foot, the next step is the extraction of ROI to perform the analysis. For this process we have split each plantar foot into six regions—the hallux or the bigger toe, other toes region (corresponding to the 2nd to the 5th toe), the plantar arch region, lateral foot region in the middle and the heel—inner and outer regions similar to that given by Hernandez-Contreras [30]. The regions are shown in Fig. 9. A bounding box is drawn around each of the foot to separate them.

For each of the regions in the bounding box, the mean temperature, the max temperature, the mean temperature difference and correlation between the corresponding regions of each foot are computed for further analysis.

5.6 Feature Extraction and Detection of Abnormality

Statistical features such as mean temperature difference (MTD) and correlation between the corresponding pixels in the left and right foot are extracted after careful processing to take into account that the left and right feet are mirror images of each other.

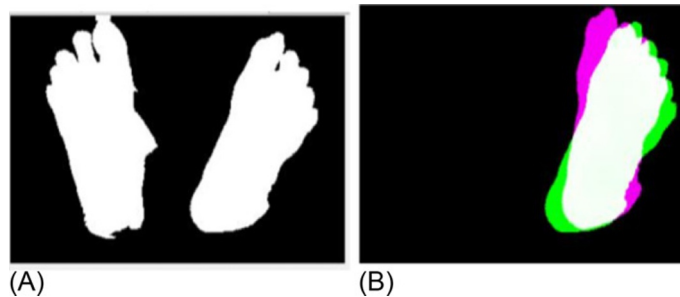


Fig. 8

(A) Segmented right and left foot and (B) registration of the left foot with respect to the right (seen in magenta color).



Fig. 9

Bounding box of the segmented left foot and the six regions of interest extracted from the bounding box. R1, big toe region; R2, other toes region; R3, plantar arch region; R4, lateral middle sole; R5, inner heel region; R6, outer heel region.

A hot region in diabetic patients is a characteristic feature of inflammation or the presence of ulcer. Fig. 10A shows the extracted hot regions as white patches. Fig. 10B shows the infrared image of a diabetic patient. The *gray color* in Fig. 10C represent cold regions. The technique followed here is thresholding. The threshold for extracting the hot region is calculated using the formula (Eq. 1).

$$\text{Max (Max Temp.of Left Foot, Max Temp of Right Foot)} \quad (1)$$

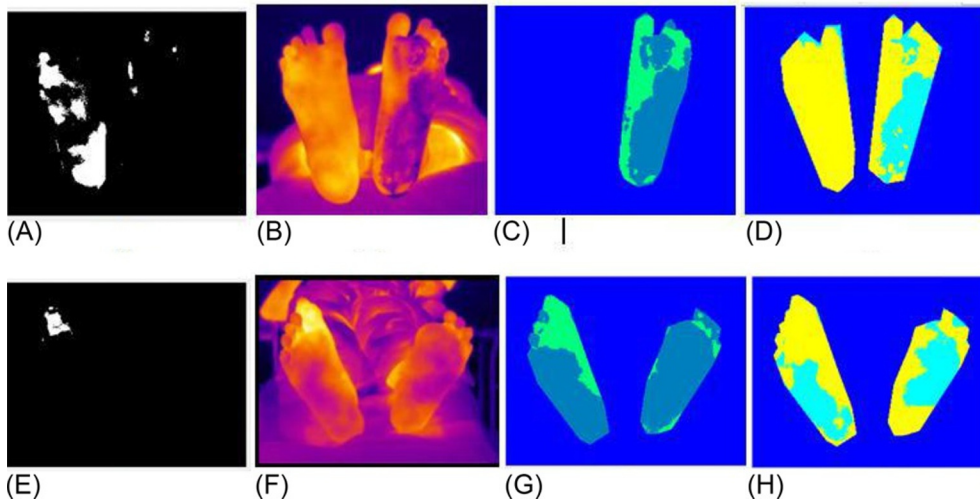


Fig. 10

(A, E) Segmented hot regions, (B, F) IR thermal image of diabetic patient, (C, G) segmented cold regions by inbuilt multilevel thresholding, and (D, H) segmented cold region using our thresholding method.

The multilevel threshold that works best for extracting the cold regions is calculated using the following formulas (Eqs. 2,3).

$$\text{Level1} = (\min (\text{Mean_LeftFoot}, \text{Mean_RightFoot})/2) \tag{2}$$

$$\text{Level2} = \min (\text{Mean_LeftFoot}, \text{Mean_RightFoot}) \tag{3}$$

The difference in the regions extracted by the built in multithresholding function and our method can be easily visualized from Fig. 10C, D and G, H.

5.7 Statistical Analysis

The features extracted are analyzed for each of the six regions. Table 2 shows the MTD for four diabetic and four healthy subjects. Table 3 shows the correlation between the corresponding left and right foot regions.

The correlation coefficient “r” is calculated between the corresponding regions (matrix A) of the left foot and right foot (matrix B) using the formula given in Eq. (4):

Table 2 Mean temperature difference (MTD) between left and right foot

S.-No.	MTD					
	R1	R2	R3	R4	R5	R6
Healthy	0.77	0.59	0.59	0.4	0.2	0.74
Healthy	0.67	0.63	0.89	0.12	0.08	0.23
Healthy	0.55	0.8	0.36	0.09	0.31	0.36
Healthy	0.81	0.732	0.35	0.85	1.14	1.13
Diabetic	0.9	0.92	0.01	0.02	0.51	1.68
Diabetic	0.32	0.24	0.3	0.02	0.38	1.75
Diabetic	3.06	0.84	1.24	0.38	0.7	3.04
Diabetic	0.24	0.26	0.17	2.72	2.65	2.42

Table 3 Correlation between left and right foot corresponding to the six regions

S.-No.	Correlation					
	R1	R2	R3	R4	R5	R6
Healthy	0.78	0.89	0.98	0.91	0.92	0.91
Healthy	0.79	0.91	0.87	0.89	0.92	0.97
Healthy	0.86	0.74	0.85	0.88	0.74	0.89
Healthy	0.8	0.92	0.64	0.89	0.78	0.95
Diabetic	0.77	0.9	0.75	0.9	0.77	0.93
Diabetic	0.72	0.84	0.77	0.95	0.81	0.94
Diabetic	0.52	0.65	0.49	0.68	0.6	0.5
Diabetic	0.61	0.7	0.63	0.5	0.42	0.46

$$r = \frac{\sum_m \sum_n (A_{mn} - \bar{A})(B_{mn} - \bar{B})}{\sqrt{\left(\sum_m \sum_n (A_{mn} - \bar{A})^2\right) \left(\sum_m \sum_n (B_{mn} - \bar{B})^2\right)}} \quad (4)$$

where \bar{A} = mean (A) and \bar{B} =mean (B).

m and n are the size of the region given as $m \times n$ pixels.

This is a valuable measure as it represents a spike in some temperature reading in the region being analyzed. Thus correlation between the left and right foot regions for diabetic subjects remain low in all the diabetic subjects analyzed. It was in the range of 0.4 to 0.8, low correlation in the region where there is an underlying complication present or building up. So this ensures that the most problematic region is not missed.

5.8 Classification of Foot for the Assessment of Diabetic Complication Using Deep Learning Neural Network

Neural networks are efficient in handling many of the issues faced by other architectures such as images corrupted by noise, degraded, and distorted images. Both similarity and dissimilarity between images can be figured out by neural nets. Also, the effective use of parallel processing can be leveraged to neural network architecture with much ease, hence reducing computation time. Features extracted from medical images are very subjective. As features are not hand crafted and learning happens in an unsupervised manner, it is very suitable to avoid any bias in reading the temperature values. Also, the ability to learn new features automatically enhances the accuracy of classification.

Deep learning is effective when we have a huge dataset which is very much limited in the case of medical domain and particularly with thermal imaging. For such small datasets, it is still possible to use Deep Convolutional Neural Networks which was pretrained on large datasets using natural images. The power of CNNs can be leveraged to small datasets using the concept of transfer learning as pointed out in Ref. [31]. We have explored the use of pretrained deep learning convolutional neural network (CNN) model called the Mobilenet model [32] to classify the foot images as healthy, diabetic without complications and diabetic with complications. Training a deep learning model from scratch will take days. But a pretrained model can be retrained for our own problem in few hours. It took just few seconds for our problem on a 1060 GPU. The evaluation/classification time taken on the machine for a single image is 0.05s on an average. We have used the Tensorflow library and the mobilenet architecture for the same. This is a preliminary study to evaluate and understand the applicability of CNN model to thermal infrared images and it has shown promising results.

Fig. 11 shows the steps involved in the using the pretrained model for our classification

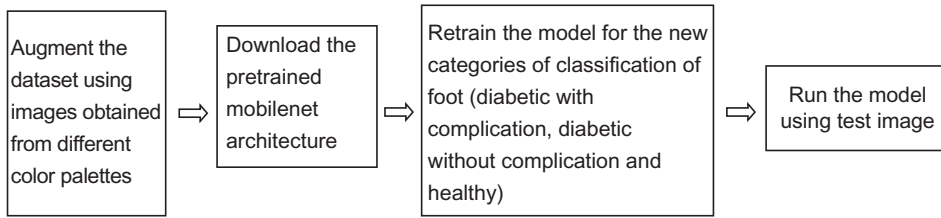


Fig. 11

Block diagram for classification using pretrained classification model.

problem. Fig. 12 shows the three classes of images that the model is trained on: the diabetic with complications, diabetic without complications and healthy subjects without diabetes.

Out of the 62 images captured from diabetic patients, 50 patients were without existing complications and 12 were with existing complications. There were 20 images in the healthy category.

Data augmentation: As this is a very small dataset, we considered augmenting the dataset with more data and since this is medical data, we cannot synthesize new data. Hence, we considered taking the different palette images for any given image. For example for a single image taken from a diabetic patient, the images in rainbow palette, hot metal, and ironbow palette were taken. Thus we have three different images for the original image. This gave a threefold increase in the number of images. Thus the total images in Diabetic without complications is 150, diabetic with complications is 36 and healthy is 60.

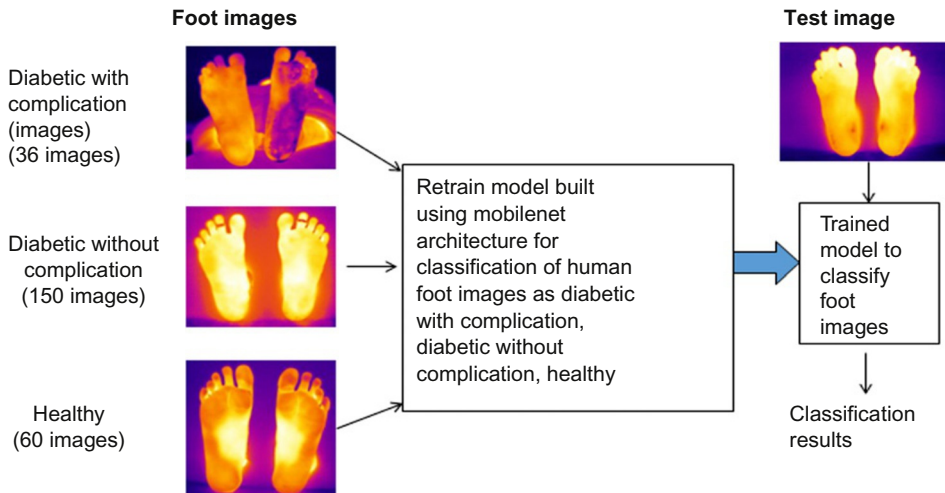


Fig. 12

The different classes of foot and the classification system.

Pretrained model used: Mobilenet architecture trained on 1000 image categories of the imagenet dataset.

Methodology used: Transfer learning—where the weight obtained in training the model on a different dataset is retrained to learn another set of classes for a different dataset (images of diabetic and healthy foot).

System configuration:

Processor: Intel core i7 processor.

Processor Speed: 3 GHz.

RAM: 16 GB.

Storage: 240 GB SSD+1 TB HDD.

Graphics card: Nvidia 1060 with 6 GB RAM.

There has been success in using various soft computing techniques such as ANN, Naïve Bayes, SVM and k-Nearest Neighbour for classification of thermograms as shown by Dey et al. [33]. The work in Ref. [34] highlights the use of convolutional neural network for segmenting the pressure areas to reconstruct the shoe last surface for designing shoes for diabetic foot.

We would be validating the results with the classification results obtained from clinical data.

6 Challenges for Medical Infrared Thermography

Even though there is a reappraisal of MIT, there are many challenges posed to this technology. The challenges are briefed in the following section.

6.1 Thermal Image Acquisition

There are no generic databases of thermal infrared images for various medical complications which are readily available for researchers to explore in comparison to visual images. Hence thermal image acquisition is a very important initial step to carry out any research on thermal infrared images.

Accurate segmentation of the ROI and hence early detection of any abnormality in the human physiology from a thermal/infrared image is possible with accurate measurement of temperature. Accurate measurement of temperature is a direct result of good quality image acquired under controlled environmental conditions which captures all the essential details required for the analysis. Hence image acquisition plays a very important role in medical image analysis. This is clearly evident in the research work presented by Sudha et al. [27] where the thermal image acquisition of foot is carried out to segment the foot from the background. In this paper, authors have analyzed three different setups for acquiring

thermal images of the foot and have discussed the influence of these on the accuracy of segmentation. The results show that acquisition protocol influences the result of image processing and hence has a pivotal role to play when it comes to efficient use of infrared thermography in medical image analysis. The thermal imager selected for the medical image analysis should have high sensitivity to pick up those minute differences in temperature that suggests an abnormality.

6.2 Environmental, Individual, and Technical Challenges

A whole lot of factors that influence the use of infrared thermography in humans have been classified in the review [26] as environmental, individual and technical factors. These factors should be taken into consideration for the effective processing of the thermal infrared images. Often it is very difficult to take care of all these factors while using infrared thermography. The most influential being the ambient temperature, relative humidity, source radiation, camera features, ROI selection, statistical analysis, medical history, metabolic rate, skin blood flow, intake factors and physical activity. Temperature measurements should ideally be accurate to within a $\pm 2\%$ margin in order to get the best results.

A detailed discussion of the challenges to medical infrared imaging is presented in Ref. [3]. Thermal reflections and occlusions are a problem with thermal infrared images. The identification and suppression of these reflections is explained in Ref. [35].

6.3 Hardware Requirements

One important factor when it comes to image processing these days which is not included in the previous set of factors is the hardware requirements. With the advancement of technology and software computing capabilities, there is a compelling need to improve the features of the underlying hardware to support high dimensionality as is the case of deep learning systems. This is becoming a basic requirement in the case of image processing using deep learning architectures. Graphical processing units (GPU) with parallel architectures are the way forward for deep learning systems built to analyze thermal images. Since deep learning is very computationally intensive, we will need a fast CPU with many cores.

6.4 Specific Challenges to Thermal Imaging

For infrared thermography to be effective the amount of heat that still exists after the heating or cooling of the object under study should also be considered.

The research challenges in medical infrared imaging are as follows:

- Stability and sensitivity of IR imaging systems.
- Understanding of body thermal patterns.

- Advanced IR image processing methods are required.
- Design of CAD systems built on soft computing techniques and efficient feature extraction methods should be explored.

7 Future Roadmap for MIT and Soft Computing

The chapter by Dey et al. [36] “Thermal imaging in medical science” gives a brief review of the current research activity in thermal imaging of breast cancer and future perspectives in MIT. Some of the recommended are

- Development of an intelligent breast thermography diagnostic system based on neural network.
- Improvement in processing, segmentation, and classification of thermal images should be carried out.
- Advancements in image fusion techniques for better understanding of thermal image is required.
- Improvement in terms of sensitivity and specificity of thermography in diagnosing various medical conditions is required.
- Automation of edge detection and object identification is still a difficult and challenging task.
- Security in transmission of thermal images has to be studied. The work by Dey et al. [37] can be considered for watermarking the images.
- Removal of noise to improve accuracy in medical diagnosis should be researched.

It is clearly evident that medical infrared thermography and soft computing will revolutionize the way healthcare is provided to people in the future. Telemedicine will also gain importance with the use of this technology. Gunes [38] studied the systems for dimensional affect recognition in multiple modalities including thermal signals represented as thermal image and found out that thermal imaging could be used to classify pretended and evoked facial expressions of positive and negative affective states.

7.1 Issues to be Addressed

Following are the issues to be addressed in building intelligent diagnostic systems by Deep-learning architectures for automated analysis of medical thermal images.

- a. Building a large database to cater to the needs of the deep learning system is difficult. So data augmentation and other techniques to synthesize data have to be evaluated and suitable technique should be considered.
- b. Gathering of expert knowledge to form the fuzzy rules for feature selection has to be carefully done to effectively classify the images.

- c. Lack of medical and bio-thermal knowledge has to be covered by discussion with medical experts.
- d. Reproducibility of the images is a great concern due to the large set of factors involved.
- e. Takes long time for the entire process from thermal image acquisition stage to the classification stage as it required repeated capturing of images in particular time gaps.
- f. Identifying the best deep learning architecture for good accuracy in classification.

8 Results and Discussion

8.1 Segmentation

The performance of the segmentation algorithm is evaluated using Jaccard index, RFN (rate of false negatives) and RFP (rate of false positives).

Jaccard index is a similarity coefficient which measures the similarity of sets based on the formula:

$$\text{Jaccard Index} = (GT \cap SI) / (GT \cup SI) \quad (5)$$

where GT represents the ground truth (manually segmented image in our case) and SI represents the segmented image (using morphological operations).

RFN and RFP is calculated using the formula

$$\text{RFN} = \text{FN} / (\text{FN} + \text{TP}) \quad (6)$$

$$\text{RFP} = \text{FP} / (\text{FP} + \text{TN}) \quad (7)$$

where FN is false negative (foreground/white pixels included as background/black pixels or omitted foreground pixels), FP is false positive (black/background pixels included as white/foreground pixels), TN is true negative (background/black pixels identified correctly) and TP is true positive (foreground/white pixels identified correctly).

The segmentation method proposed here and performance evaluation of the method is implemented in MATLAB R2016a. The evaluation of our segmentation method for 15 diabetic subject images based on the three measures is given in [Table 4](#).

From [Table 4](#), it can be observed that the segmentation of the foot from the background is comparable with the ground truth. But there is still scope for reducing the False Positives, False Negatives, and the Jaccard Index. High FPs is a result of white pixels which should not be part of the segmented result as in the case of image 3 in the table. This is because the toes are cold and the temperature of the background matches with the other part of the foot and hence it becomes part of the segmented image making the count of white/foreground pixels to increase. Also, FNs in image 8 is high because of cold foot with temperatures merging with the background. Thus, the count of black/background pixels increase which

Table 4 Performance of the segmentation method

Images S.No	Performance of the Proposed Segmentation Method		
	Jaccard Index	RFP	RFN
1	0.9254	0.0128	0.0035
2	0.9462	0.0246	0.0152
3	0.6812	0.852	0.623
4	0.8483	0.0823	0.0875
5	0.9715	0.0265	0.0123
6	0.8212	0.082	0.0537
7	0.9682	0.0116	0.0098
8	0.7128	0.2104	0.1342
9	0.9754	0.0323	0.0145
10	0.9856	0.0154	0.0032
11	0.9422	0.0887	0.0784
12	0.9204	0.0375	0.0196
13	0.8573	0.1280	0.0278
14	0.9345	0.0284	0.0173
15	0.9041	0.0679	0.0450

contribute to higher FN's. To improve the accuracy further, we are planning to explore the use of deep learning for the segmentation task also.

8.2 Statistical Analysis of the Surface Temperature Distribution (STD) to Detect Abnormality

The outcome of the analysis done is as follows:

- The STD is symmetrical across all the corresponding regions in left and right foot in healthy subjects.
- The temperature is considerably high at the region 3 (plantar arch) owing to the butterfly pattern and is at least 1.5°C higher compared to the other regions for a particular foot. This is vice versa in the case of patients with diabetic foot complications where the temperature was higher in the region of complication.
- The temperature difference of 2.2°C was observed in the presence of foot complication.
- Correlation coefficients between the left and right foot is >0.8 in the case of healthy subjects and it is less in the range of 0.4 to 0.7 in most of the diabetic subjects. Since this range is mutually exclusive between the diabetic and healthy subjects, correlation coefficient is a very good indicator of abnormal thermal pattern. When the patient has good diabetic control, then the correlation is equivalent to that of healthy subject as can be seen in the first two diabetic subjects in [Table 3](#).
- The right foot had the maximum temperature in the regions 1, 2, and 3 compared to the left foot in all the subjects both healthy and diabetic. This explains why right foot is the most common site for diabetic foot problems.

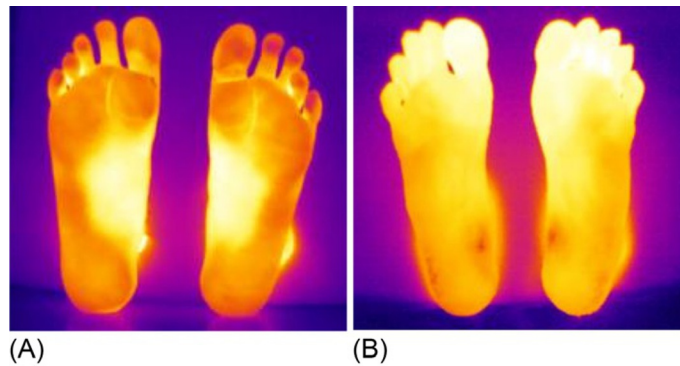


Fig. 13

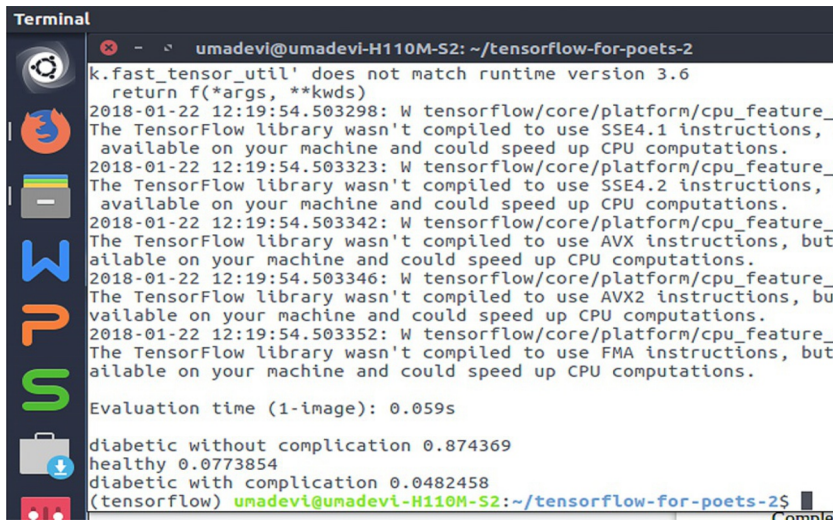
Foot thermal images showing (A) butterfly pattern in healthy subject and (B) absence of butterfly pattern and presence of hyperthermia in the toes region of diabetic subject.

Plantar foot temperature varies in diabetic foot due to thermoregulation problems related to neuropathy and/or ischemia, and also in case of inflammation. There is a wider variation in diabetic patients compared to healthy subjects. Region 3 shows the maximum temperature in two nondiabetic subjects as expected in the arch region where a butterfly pattern is a characteristic of healthy foot as shown in Fig. 13.

There was significant difference in temperature in the regions corresponding to each foot whenever there is an abnormality. Registration is approximate in the sense that when the big toe is amputated, the bounding box heights differ and hence the regions are not properly segmented. The hot and cold regions extracted from the images suggest the location of an underlying inflammation or the extent of inflammation if present already in the case of ulcer or the presence of neuropathy. The isolation of these regions will help the doctor in identifying the underlying angiosome for assisting in therapy or surgery. The dataset used is small and it has to be built with more images so that the analysis is more accurate. The next step is to build such a dataset. Segmentation of the foot from the background posed problems in the case of diabetic patients when the toes were cold. Hence we are looking forward to build a deep learning network to do the segmentation.

8.3 Classification of Foot Using Transfer Learning of Pre-trained CNN Model

A typical output from the classification of a test image using the CNN classifier is shown in Fig. 14. This shows that the image given to the model is classified as a diabetic foot without any complication with a probability of 87.43% which is very high compared to the next two predictions which is healthy with 7.73% and diabetic with complication with 4.82%. This clearly shows that the model is able to distinguish between different categories with greater confidence. This prediction is correct for the given image. Similarly by testing all the images, we got an average accuracy of 91% for each of the classes. This is really amazing given the fact



```

Terminal
umadevi@umadevi-H110M-S2: ~/tensorflow-for-poets-2
k.fast_tensor_util' does not match runtime version 3.6
return f(*args, **kwargs)
2018-01-22 12:19:54.503298: W tensorflow/core/platform/cpu_feature_
The TensorFlow library wasn't compiled to use SSE4.1 instructions, b
available on your machine and could speed up CPU computations.
2018-01-22 12:19:54.503323: W tensorflow/core/platform/cpu_feature_
The TensorFlow library wasn't compiled to use SSE4.2 instructions, b
available on your machine and could speed up CPU computations.
2018-01-22 12:19:54.503342: W tensorflow/core/platform/cpu_feature_
The TensorFlow library wasn't compiled to use AVX instructions, but
available on your machine and could speed up CPU computations.
2018-01-22 12:19:54.503346: W tensorflow/core/platform/cpu_feature_
The TensorFlow library wasn't compiled to use AVX2 instructions, but
available on your machine and could speed up CPU computations.
2018-01-22 12:19:54.503352: W tensorflow/core/platform/cpu_feature_
The TensorFlow library wasn't compiled to use FMA instructions, but
available on your machine and could speed up CPU computations.

Evaluation time (1-image): 0.059s

diabetic without complication 0.874369
healthy 0.0773854
diabetic with complication 0.0482458
(tensorflow) umadevi@umadevi-H110M-S2:~/tensorflow-for-poets-2$

```

Fig. 14

Output of the classifier for the test image of a diabetic patient without complication.

that thermal imaging is totally different from any other imaging modality and the model is pretrained on natural images (~1,42,000 images).

This preliminary study assures us that we could use deep learning for our problem also. We are planning to build such a model from scratch to have more control over the parameters to fine tune the classification and to quantify the level of complication as different categories.

9 Future Research Directions on Diabetic Foot Assessment

In the days to come our focus would be on the following:

- Explore the use of deep learning for segmentation of the foot from background.
- Build a mathematical classification model based on the quantification of risk of ulcer formation.
- Build a software system using all the image processing and classification work carried out for the early diagnosis and quantification of the diabetic foot complications.
- Correlate with the existing clinical foot evaluation methods to evaluate the system built and its applicability for use as a home monitoring tool for diabetic foot.
- Develop a mobile application capable of using as an adjunct tool for telemedicine and home monitoring of diabetic foot complication.

10 Conclusion

Medical Infrared Thermography being noninvasive and noncontact has the special ability to diagnose human physiology due to heat transfer in skin tissues. With the special characteristics

and advantages of thermal imaging, computer aided diagnosis systems are becoming more and more accurate and effective. The advancements in image processing, feature extraction and selection and soft computing techniques like deep learning in combination with improvements in parallel computing architectures have paved way for more interest and importance to research in this imaging modality. The soft computing techniques used mostly are artificial neural networks, SVM and genetic algorithm with texture based features for most of the classification task. But the most effective ones are the mean temperature difference and correlation. With more computing power and capability of the recent systems and the reappraisal of thermography in medicine, we shall see more advances in deep learning in the years to come. Thermography is being recognized as an adjunct tool for detecting abnormality in the temperature profile of patients to uncover an underlying disease or inflammation. The advantage of being noncontact and noninvasive makes it a safe diagnostic imaging technique. This chapter emphasizes the use of existing soft computing techniques coupled with the specific characteristics of infrared thermography making it more efficient and safe. The authors' current work on automated foot thermal image analysis for diabetic foot assessment is also discussed and future research directions are also given.

Acknowledgments

The work reported in this chapter is supported by the college (BMS College of Engineering) through Technical Education Quality Improvement Programme [TEQIP-III] of the MHRD, Government of India by providing the thermal camera for this research. We are also thankful to Al-Amoudi Scientific Research Foundation (ASRF) for providing funds for setting up GPU computing facility in the college. We are also very grateful to the podiatric surgeon at KIER, Dr. B. Pavan for his valuable input in collecting patient details and to all the patients who consented to participate in this study.

References

- [1] J. Jiang, E.Y.K. Ng, A.C.B. Yeo, S. Wu, F. Pan, W.Y. Yau, J.H. Chen, Y. Yang, A perspective on medical infrared imaging, *J. Med. Eng. Technol.* 29 (6) (2005) 257–267.
- [2] A. Szentkuti, H.A.N.A.S. Kavanagh, G. Simeon, *Infrared thermography and image analysis for biomedical use*, *Period. Biol.* 113 (4) (2011) 385–392.
- [3] M. Diakides, J.D. Bronzino, D.R. Peterson (Eds.), *Medical Infrared Imaging: Principles and Practices*, CRC Press, Taylor & Francis Group, Boca Raton, FL, 2013.
- [4] Y. Houdas, E.F.J. Ring, *Human Body Temperature*, Plenum Press, New York, 1982.
- [5] E.F.J. Ring, The historical development of temperature measurement in medicine, *Infrared Phys. Technol.* 49 (2007) 297–301.
- [6] J.D. Hardy, The radiation of heat from the human body. I–IV, *J. Clin. Invest.* 13 (1934) 593–620 and 817–883.
- [7] J.D. Hardy, C. Muschenheim, The radiation of heat from the human body V, *J. Clin. Invest.* 15 (1936) 1–8.
- [8] F. Ring, A. Jung, J. Žuber, *Infrared Imaging*, IOP Publishing, 2015. ISBN: 978-0-7503-1143-4.
- [9] B.B. Lahiri, S. Bagavathiappan, T. Jayakumar, J. Philip, Medical applications of infrared thermography: a review, *Infrared Phys. Technol.* 55 (2012) 221–235.
- [10] V. Umadevi, S.V. Raghavan, S. Jaipurkar, Framework for estimating tumour parameters using thermal imaging, *Indian J. Med. Res.* 134 (5) (2011) 725–731, <https://doi.org/10.4103/0971-5916.91012>.
- [11] N. Padmapriya, N. Venkateswaran, T. Kannan, M. Sindhumathuri, Assessment of Glaucoma with ocular thermal images using GLCM techniques, in: 12th International Conference on Quantitative Infrared

- Thermography, Mamallapuram, India, 2015 (Published online in QIRT Open-Archives at <http://qirt.org/archives/qirtasia2015doi/papers/CP0098.pdf>).
- [12] B.F. Jones, P. Plassmann, Digital infrared thermal imaging of human skin, *IEEE Eng. Med. Biol. Mag.* 21 (6) (2002) 41–48.
 - [13] L.I. Izhar, Registration and Analysis of Thermal Images in Medicine (PhD dissertation), Imperial College London, 2014.
 - [14] U. Oliver Faust, E.Y.K. Rajendra Acharya, T.J.H. Ng, W. Yu, Application of infrared thermography in computer aided diagnosis, *Infrared Phys. Technol.* 66 (September) (2014) 160–175.
 - [15] C.L. Herry, M. Frize, Quantitative assessment of pain-related thermal dysfunction through clinical digital infrared thermal imaging, *Biomed. Eng.* 3 (2004) 19, <https://doi.org/10.1186/1475-925X-3-19>.
 - [16] N. Dey, A.S. Ashour, F. Shi, V.E. Balas (Eds.), *Soft Computing Based Medical Image Analysis*, Academic Press, Cambridge, Massachusetts, 2018. ISBN: 9780128130872.
 - [17] S. Bagavathiappan, J. Philip, T. Jayakumar, B. Raj, P.N.S. Rao, M. Varalakshmi, V. Mohan, Correlation between plantar foot temperature and diabetic neuropathy: a case study by using an infrared thermal imaging technique, *J. Diabetes Sci. Technol.* 4 (6) (2010) 1386–1392.
 - [18] P.I. Brånemark, S.E. Fagerberg, L. Langer, J. Säve-Söderbergh, Infrared thermography in diabetes mellitus a preliminary study, *Diabetologia* 3 (6) (1967) 529–532.
 - [19] M. Bharara, J.L. Mills, K. Suresh, H.L. Rilo, D.G. Armstrong, Editorial: diabetes and landmine-related amputations: a call to arms to save limbs, *Int. Wound J.* 6 (1) (2009) 2–3.
 - [20] H. Peregrina-Barreto, L.A. Morales-Hernandez, J.J. Rangel-Magdaleno, J.G. Avina-Cervantes, J.M. Ramirez-Cortes, R. Morales-Caporal, Quantitative estimation of temperature variations in plantar angiosomes: a study case for diabetic foot, *Comput. Math. Methods Med.* 2014 (2014) Article ID 585306, 10 pages (1–10).
 - [21] D. Hernandez-Contreras, H. Peregrina-Barreto, J. Rangel-Magdaleno, J.A. Gonzalez-Bernal, L. Altamirano-Robles, A quantitative index for classification of plantar thermal changes in the diabetic foot, *Infrared Phys. Technol.* 81 (2017) 242–249.
 - [22] C. Liu, J.J. van Netten, J.G. Van Baal, S.A. Bus, F. van Der Heijden, Automatic detection of diabetic foot complications with infrared thermography by asymmetric analysis, *J. Biomed. Opt.* 20 (2) (2015) 026003.
 - [23] F.-J. Renero-C, The abrupt temperature changes in the plantar skin thermogram of the diabetic patient: looking in to prevent the insidious ulcers, *Diabet. Foot Ankle* 9 (1) (2018) 1430950, <https://doi.org/10.1080/2000625X.2018.1430950>.
 - [24] A. Gatt, et al., Establishing differences in thermographic patterns between the various complications in diabetic foot disease, *Int. J. Endocrinol.* 2018 (2018) Article ID 9808295, 7 pages (1–7).
 - [25] D. Hernandez-Contreras, H. Peregrina-Barreto, J. Rangel-Magdaleno, J. Gonzalez-Bernal, Narrative review: diabetic foot and infrared thermography, *Infrared Phys. Technol.* 1350-449578 (2016) 105–117, <https://doi.org/10.1016/j.infrared.2016.07.013>.
 - [26] I. Fernández-Cuevas, et al., Classification of factors influencing the use of infrared thermography in humans: a review, *Infrared Phys. Technol.* 71 (2015) 28–55.
 - [27] B.G. Sudha, V. Umadevi, J.M. Shivaram, Thermal image acquisition and segmentation of human foot, in: 4th International Conference on Signal Processing and Integrated Networks (SPIN), Noida, 2017, pp. 80–85, <https://doi.org/10.1109/SPIN.2017.8049920>.
 - [28] T.F. Chan, L.A. Vese, Active contours without edges, *IEEE Trans. Image Process.* 10 (2) (2001) 266–277.
 - [29] S.E. Zohora, S. Chakraborty, A.M. Khan, N. Dey, in: Detection of exudates in diabetic retinopathy: a review, 2016 International Conference on Electrical, Electronics, and Optimization Techniques (ICEEOT), Chennai, 2016, pp. 2063–2068, <https://doi.org/10.1109/ICEEOT.2016.7755052>.
 - [30] D. Hernandez-Contreras, H. Peregrina-Barreto, J. Rangel-Magdaleno, J. Ramirez-Cortes, F. Renero-Carrillo, Automatic classification of thermal patterns in diabetic foot based on morphological pattern spectrum, *Infrared Phys. Technol.* 73 (2015) 149–157.
 - [31] G. Litjens, et al., A survey on deep learning in medical image analysis, *Med. Image Anal.* 42 (2017) 60–88.
 - [32] C. Szegedy, et al., in: Rethinking the inception architecture for computer vision, Proceedings of the IEEE Conference on Computer Vision and Pattern Recognition, 2016.
 - [33] N. Dey, A.S. Ashour, S. Borra (Eds.), Classification in BioApps: Automation of Decision Making, In: vol. 26, Springer, Cham, 2017.

- [34] Z. Li, N. Dey, A.S. Ashour, L. Cao, Y. Wang, D. Wang, F. Shi, Convolutional neural network based clustering and manifold learning method for diabetic plantar pressure imaging dataset, *J. Med. Imaging Health Inform.* 7 (3) (2017) 639–652.
- [35] S. Henke, D. Karstädt, K.-P. Möllmann, F. Pinno, M. Vollmer, Identification and suppression of thermal reflections in infrared thermal imaging, *Inframation Proc.* 5 (2004) 287–298.
- [36] N. Dey, A.S. Ashour, A.S. Althoupey, Thermal imaging in medical science, in: *Recent Advances in Applied Thermal Imaging for Industrial Applications*, IGI Global, 2017, pp. 87–117. Web. 26 Feb. 2018, <https://doi.org/10.4018/978-1-5225-2423-6.ch004>.
- [37] N. Dey, S.S. Ahmed, S. Chakraborty, P. Maji, A. Das, S.S. Chaudhuri, Effect of trigonometric functions-based watermarking on blood vessel extraction: an application in ophthalmology imaging, *Int. J. Emb. Sys.* 9 (1) (2017) 90–100.
- [38] H. Gunes, Automatic, dimensional and continuous emotion recognition, *Int. J. Synt. Emot.* 1 (1) (2010) 68–99.